Available online at www.sciencedirect.com

ScienceDirect

Procedia CIRP 81 (2019) 820–825

www.elsevier.com/locate/procedia

52nd CIRP Conference on Manufacturing Systems

Compensation of part distortion in process design for re-contouring processes

Volker Böß[a], Felix Rust[a,]*, Marc-André Dittrich[a], Berend Denkena[a]

[a]*Institute of production engineering and machine tools, An der Universität 2, 30823 Garbsen*

* Corresponding author. Tel.: +49-511-762-18069; fax: +49-511-762-5115. *E-mail address:* rust@ifw.uni-hannover.de

Abstract

The repair of compressor blades requires a precise coordination of the material deposit and the subsequent re-contouring process. Since re-contouring is the last step in the process chain, it is a crucial stage for the final part quality and shape. Therefore, machining-induced part distortions must be considered in process design. This paper introduces a method for the simulation-based compensation of part distortions. The method combines process planning and evaluation by means of a geometric simulation. In order to validate the approach, milling experiments are carried out. A subsequent measurement of the part geometry shows that the part distortion can be reduced by up to 21% using the presented approach.

Keywords: part distortion; milling; blade repair; adaptive manufacturing

1. Introduction

The MRO (Maintenance, Repair and Overhaul) market expects a growth rate of 4.1% per year until 2025. Especially the annual spending in the sectors “engine repair” and “engine overhaul” is going to increase about $13.7 billion each year. Therefore, aerospace companies will allocate more of their financial resources to new MRO technology [1]. This includes innovation and automation of repair processes for turbine blades. In most cases, the repair process consists of the following steps: pre-inspection, geometric reconstruction, material deposit (laser welding or patch welding), re-contouring (machining) and post-inspection.

Re-contouring, e.g. by milling, is defined as the restoration of the former shape of the part. Consequently, it determines the final part geometry and surface quality. Because of the strict safety regulations in engine repair, tight tolerance must be met by the re-contouring process. [2–4]. At the same time, the repair of damaged blades or vanes is highly specific, due to thermic induced creeping during engine operation and individual damages.

At the beginning of the repair process, the individual target shape of the part must be known. For that purpose, the blade is virtually reconstructed by reverse engineering (RE) using methods from computer-aided design (CAD). This task is automatized for damages in the mid profile height of blades [5–7]. For the subsequent material deposit, laser welding is increasingly used as this process causes less heat input into the material than conventional welding technologies [5, 8–11]. Afterwards, machining operations are used for restoring the shape of the blade. In re-contouring, the cutting parameters affect the part quality and the resulting performance of the blade as well [2,12,13]. E.g. in repair of thin-walled blades, the process-induced residual stresses cause part distortions. Wang and Sun examine the impact of residual stresses on the blade shape after milling and prove that form errors result due to residual stresses [14]. In order to predict residual-stresses-induced part distortion,

10.1016/j.procir.2019.03.206

finite element analyses (FEA) are suitable [15]. For the prognosis, the distortion stemming from machining is mostly reduced to an elastic-plastic body deformation due to external loads. Like Zhan et al. show in their FE approach, a fairly good prognosis of part distortion is possible. Nevertheless, the load due to machining force or residual stresses must be known in advance [16]. Moreover, meshing and re-meshing of the part geometry is needed when the part geometry changes. Due to individual repair cases in re-contouring and the consequential varying engagement conditions, FEA is not feasible from a practical point of view. An alternative is the prognosis based on geometric cutting conditions. Regarding the prognosis of residual stresses in five-axis ball-end milling of Ti-6Al-4V, Denkena et al. have introduced the idea of surface generating forces. These are material dependent and relate to the cutting volume that directly forms the surface [17]. A parameter to describe residual stresses in the simulation is also useful for the evaluation of part distortion in the machining of simple plates. Consequently, the approach may allow to model the resulting part distortion in compressor blade re-contouring and adjust the process planning accordingly.

In the first part of the article, a novel approach for the compensation of part distortions in milling thin-walled blades based on the surface-generating cut volume (SGCV) is introduced. The second part explains the experimental investigation of the presented approach in 5-axis milling.

2. Compensation approach

In re-contouring, if the process planning, process or machine behavior contains only small errors the valuable blade turns a scrap part afterwards. This is the reason why process time is of secondary importance and an increase of material removal rate is not intended. Presented compensation approach only considers part quality in terms of final part shape. Shape error caused by tool deflection in milling compressor blades has been addressed in another work [18]. Part distortion is invoked by locally induced residual stresses [17] but have global impact on part shape after unclamping the blade. Thus, it is a crucial task to reduce part distortion by adjusted processes.

In order to reduce part distortion, it is necessary to minimize the residual stresses induced by machining. For that purpose, the compensation method must include three tasks. First, the method must allow the evaluation of the part distortion by means of a given tool path and process parameters. Second, the method should be able to derive suitable parameters that minimize process-induced residual stresses. Finally, the developed method must provide an individual tool path for each blade. In the following sections, all three elements and their interactions are presented.

2.1. Evaluation of part distortion

In order to avoid aforementioned problems of FE simulations, the part distortion is evaluated by the SGCV, which is obtained from a geometrical cutting simulation using IFW CutS [19]. The SGCV represents the cut volume that is removed by the tool while forming the final surface (see Fig. 1, bottom). Hence, the SGCV represents a fraction of the uncut chip thickness. Taking into account surface generating forces (SGF), which observe the chip thickness and the generated surface, the induced residual stresses can be predicted [20]. It has been shown in an earlier work by the authors that the SGCV correlates positively with the part distortion induced by residual stresses in re-contouring thin plates made of Ti-6Al-4V (see Fig. 1). Furthermore, the presented results reveal a high influence of lead and tilt angle on the resulting residual stresses and part distortion.

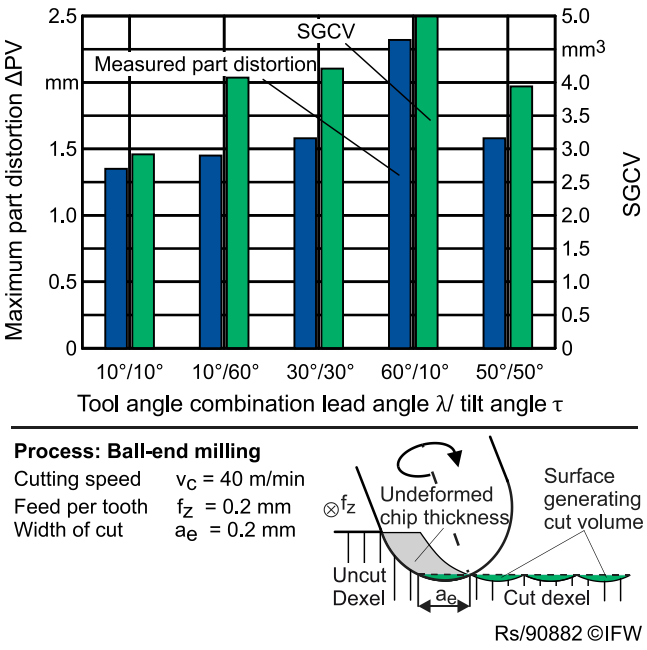

Fig. 1. Correlation between maximum part distortion and simulated SGCV.

The correlation of experimental results and the simulation parameter SGCV lead to the idea of compensating part distortion via adapting process parameters depending on SGCV. Hence, the presented method is based on a look-up table approach that connects the process parameter tool angle with the simulated SGCV. In order to generate a look-up table (called SGCV matrix in the following) simulations have been carried out with varying lead and tilt angle. The surface size (1 mm²) was kept constant as well as the feed rate (0.2 mm), the radial engagement (0.2 mm) and the axial engagement of the tool (30 µm). Lead and tilt angles were varied between +10° and +60° respectively. The SGCV was simulated for each resulting tool angle combination. Fig. 2 depicts the resulting SGCV matrix as a three dimensional plot. It does not describe the absolute part distortion. Rather it connects induced part distortion with each angle combination. Hence the look-up table allows a selection of process parameters with a specific SGCV.

A limiting boundary condition is the poor accessibility of the re-contouring area, which is a common problem that occurs in the repair of blade integrated disks (blisks). Furthermore, the damages on both sides of the blade area are different in size. Therefore, the idea is to provide a process parameter selection guide for the re-contouring of blades.

The process planning and parameter selection, described in the next section, have been tested for this scenario. The method in question considers the finishing process only.

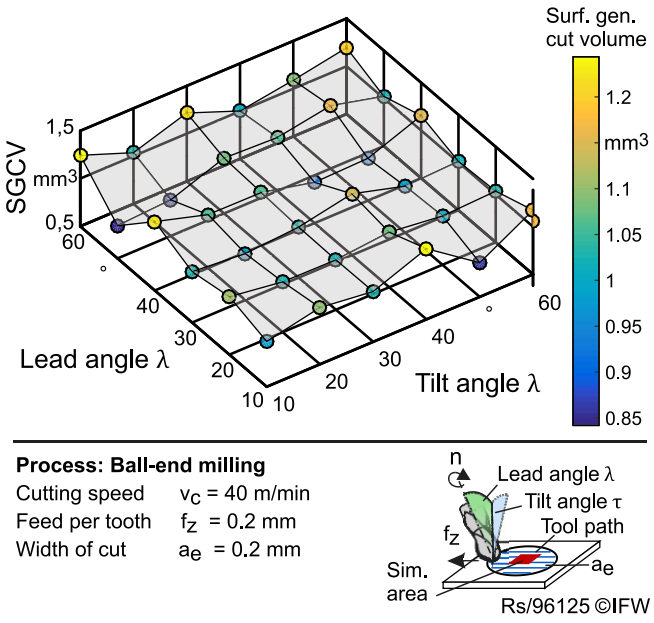

Fig. 2. SGCV matrix for the given process. Points represent single simulations. The grid is depicted only for orientation for the reader.

2.2. Process planning

2.2.1. Process parameter selection

Fig. 3 summarizes the approach for selecting suitable process parameters of the re-contouring process. Based on external constraints (e.g. accessibility), an initial tool path is calculated by a CAM software. The path includes initial parameters (λ_{init} and τ_{init}). These are input parameters for the method in order to find optimal tool angles for both sides of the blade. Hence, for parameter selection the blade is simplified by two surfaces, called surface 1 and surface 2 in the following pages. The first step is determining the SGCV matrix for surface 1. This is achieved by multiplying the area of surface 1 by the initial SGCV matrix, which has been simulated for an area of 1 mm² (see section 2.1). The SGCV matrix for surface 1 represents the surface-generating cut volume that forms throughout the re-contouring of surface 1 using different tool angle combinations. With the initial lead and tilt angle the value SGCV1 is determined. SGCV1 represents the local minimum of SGCV for surface 1 within a specific search radius around λ_{init} and τ_{init}. The search radius is set to 10° in this case. This results in the tool angles λ1 and τ1 for surface 1. The value is defined by the scope in which the re-contouring is possible at the associated position of the blade regarding potential collision of the tool. Afterwards, the SGCV matrix for surface 2 is calculated equivalent to surface 1. For the determination of the tool angles at surface 2, a local minimum of the difference between SGCV1 and SGCV2 must be found within the search radius. In order to compensate the part distortion, the difference of both SGCV must lie near zero. The resulting minimum ΔSGCV leads to the angles λ2, τ2 for surface 2.

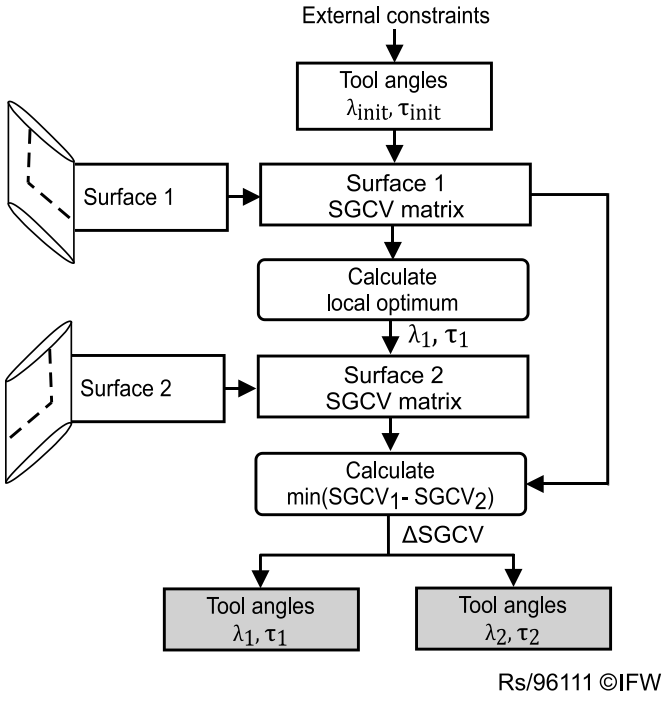

Fig. 3. SGCV-based process-parameter selection.

For the identification of the limits of the described parameter-selection method, four different theoretical area sizes for surface 1 and the associated area sizes for surface 2 have been selected. For each area pair, the best angle pair has been determined using the method in Fig. 3. The corresponding difference in SGCV1 and surface ratio of both areas are shown in Fig. 4.

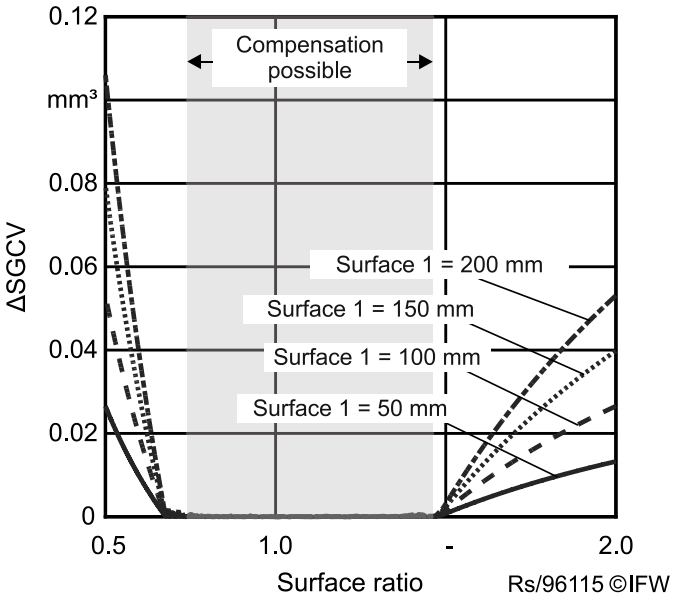

Fig. 4. Difference between $SGCV_1$ and $SGCV_2$ compared to surface area ratio for theoretical values of surface area 1.

It can be seen that upper and lower surface ratio boundaries exist that allow a mutual compensation of SGCV on both sides of the blade. These are 0.75 and 1.45

respectively. Therefore, the induced residual stresses difference on both sides leads to an uncompensated blade.

The resulting tool angles for both surfaces serve as input for the generation of the individual tool path, as described in the next section.

2.2.2. Tool path modification

After selection of the tool angles, the initial tool path is adapted to the individual blade. For that purpose, an algorithm for the automatic modification of the initial tool path is developed (see Fig. 5). The algorithm uses an interface to a CAM system and self-developed post-editing methods for CLSF-based (CLSF – cutter location source file) program descriptions.

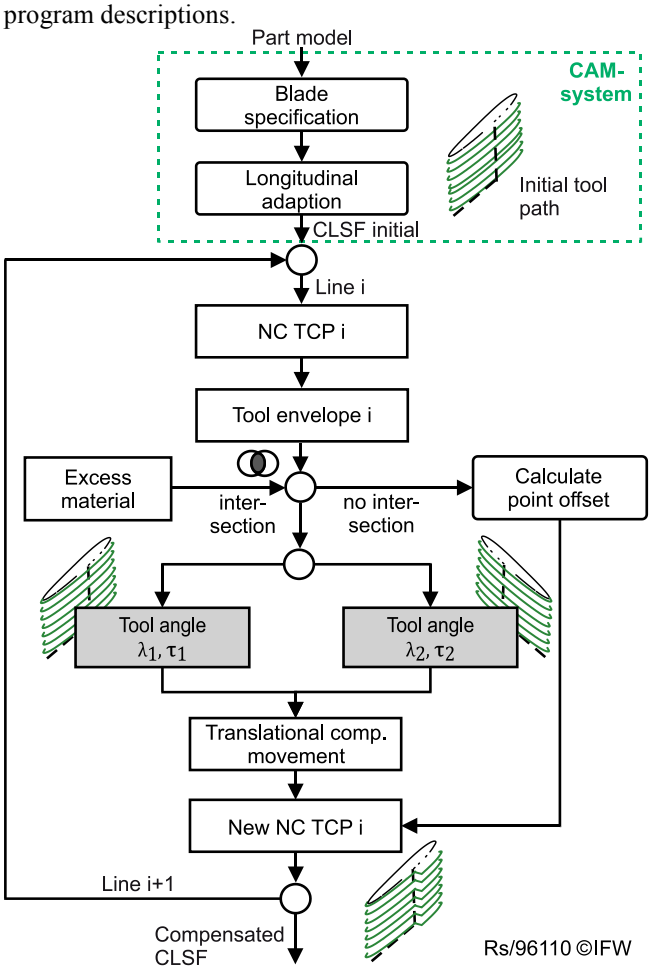

Fig. 5. Tool path modification for the compensation of the two-sided re-contouring process of a part distortion.

The modification of the initial tool path starts with trimming in longitudinal direction of the blade until the lowest excess material. The tip of the blade defines its highest point. This step is carried out within the CAM system. The CLSF of the initial tool path consists of all cutter location points of the process (CLP), referring to the tool center point.

The CLSF is subsequently modified based on the tool envelope i for each CLP as well as the volumetric dexel discretization of the blade and the excess material. For each CLP, a boolean operation is applied to the appropriate tool envelope and the excess material. If an intersection is registered, the tool is re-contouring one of the two surfaces. In this case, the tool angle is modified for its optimization. Afterwards, the CLP is modified by adding a translational compensation movement to keep the tool contact on the blade surface after changing the tool angle. This leads to a new TCPi. If no intersection is registered, an offset in tool axis direction is added to the CLP.

This method has shown a reduced axis movement in the re-contouring process. But more importantly, it increases process safety regarding tool collisions, as the initial tool path is only minimally modified. However, a collision-free-template tool path and mainly uniform-clamping conditions of the blades are necessary. The downstream tool path modification is not necessarily required for the compensation of part distortion. It rather provides defined steps for a safe and automatic implementation of the previously selected tool angles.

3. Experimental re-contouring of a blade

In order to examine the efficiency of the above described method, analogy blades have been re-contoured experimentally. The blades were manufactured through milling. The additional excess material was modelled within the milling process as well. The profile of the blade is derived from a blisk profile, which presents an equal extrusion from the center cross section of the blade . This leads to a blade profile with zero twist angles for the blade (see Fig. 6 a). The blade material is Ti-6Al-4V. In order to simulate excess material, each side of the blade contains a circular survey of different sizes.

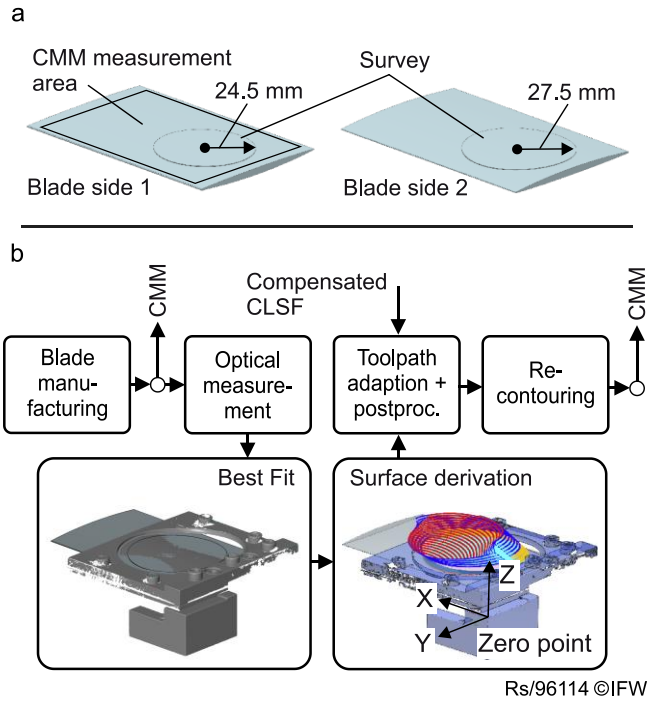

Fig. 6. (a) Analog blade and (b) experimental procedure.

The sizes were 24.5 mm (surface 1) and 27.5 mm (surface 2), resulting in a surface ratio of 1.26.

The milling of the blade was conducted on a 5-axis milling center DMU 125P. After milling, a stress relief heat treatment in a vacuum oven was carried out by the Institute of Materials Science at the Leibniz University Hannover (IW). The manufacturing of the blade resulted in production tolerances. These tolerances had to be taken into account in the subsequent re-contouring process and were filtered out in the later experimental analysis.

The milling of thin-walled parts contains high risk of workpiece vibrations. Hence, in industrial manufacturing and re-contouring a dividing head is used for blade clamping. As a divider was not accessible on the machine tool, an alternative approach for blade clamping was necessary. In this regard, a two-piece clamping device was developed, including a cartridge and a cover. These provide a clutching of the blade on both sides. Both parts include circular open pockets in areas where the circular surveys were located. For process planning, the two-piece clamping, including the clamped blade, was mounted with screws on a fixture. In order to reference the blade position with regard to the actual clamping, the whole assembly was scanned with an optical measurement system GOM ATOS Core 200 using light stripe projection (see Fig. 6 b).

The scanned assembly was best-fit with the CAD model of the blade. The actual surface area (point cloud) was transferred into a NURBS surface using Siemens NX and the zero point was defined on the scanned corner of the fixture. The compensated CLSF was then adapted to the actual surface. For experimental analysis, the blade was measured with a coordinate measuring machine (CMM) after manufacturing and after re-contouring. In order to show the potential of the method, four blades were manufactured and re-contoured. This resulted in one experiment and one retry for each process strategy.

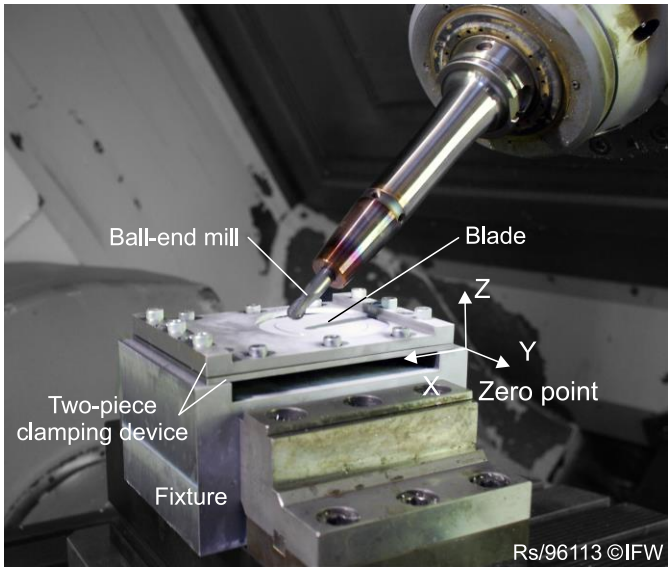

Fig. 7. Experimental setup.

For all experiments, a two-fluted ball end mill with rounded cutting edges was used. The coated ball end mill SECO Jabro Tornado had a diameter of 10 mm. Blade 1 and 2 were re-contoured using a conventional strategy with constant tool angles over the entire blade. These are a lead angle of $\lambda_1 = 50°$ and a tilt angle of $\tau_1 = 10°$. The tilt and lead angles for the compensated blades (blade 3 and 4) were chosen in a way that the value for ΔSGCV was near zero (see section 2.2.1). This resulted in lead and tilt angles of $\lambda_1 = 50°$ and $\tau_1 = 10°$ respectively for surface 1. For surface 2 the lead angle is $\lambda_1 = 30°$ and the according tilt angle is $\tau_1 = 50°$.

4. Results and discussion

For the experimental analysis, both the probed points of the CMM measurement of the manufactured blades and the re-contoured blades were taken into account. The blades were probed within a grid of 19 x 29 points on one side of the blade, resulting in a total of 551 measuring points. As only the blade distortion was examined, the re-contouring area has been excluded from the analysis. In order to analyze re-contouring-induced part distortion, measuring points before and after re-contouring were subtracted from each other. After re-contouring, all blades showed a qualitatively similar distribution of part distortion. The point clouds, shown in Fig. 8 a and b, represent the average of the two experiments for each process, conventional and compensated strategy.

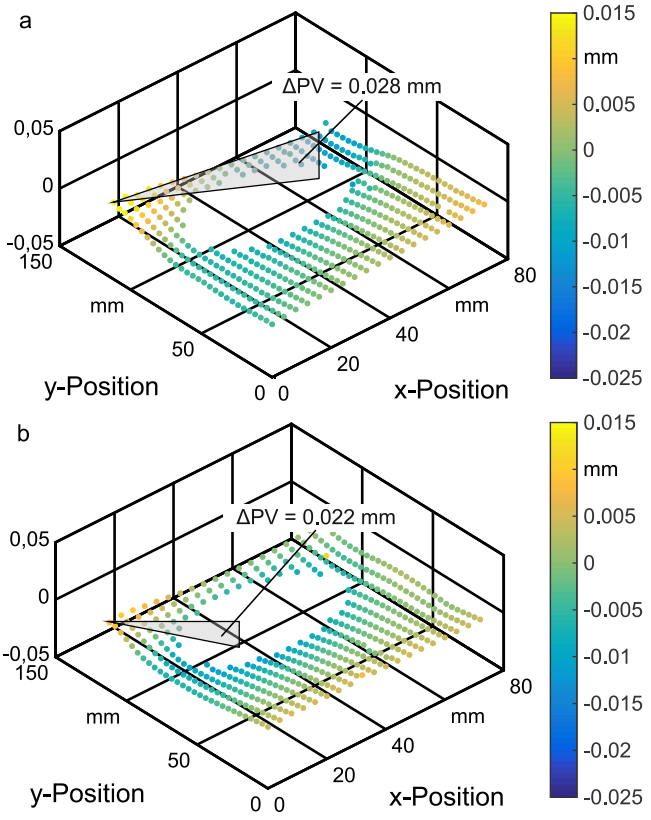

Process: Ball-end milling

v_c = 40 m/min
a_e = 0.2 mm
f_z = 0.2 mm

a) λ = 50°, τ = 10 °
λ = 50°, τ = 10 °
b) λ = 50°, τ = 10 °
λ = 30°, τ = 50 °

Rs/96112 ©IFW

Fig. 8. Comparison of the measured part distortion of (a) the uncompensated and (b) the compensated blade.

Results reveal part distortions defined by the blade side with the larger re-contouring area (see Fig. 6 a). The compressive residual stresses result in a contraction of the sub-surface on that side. That explains the convex shape on the opposite side of the blade with the smaller re-contouring area.

The remaining distortion is caused by the following circumstances. Due to the production tolerances, the positions of the circular surveys were different. The applied method is based on the idea that internal loads (residual stresses) that cause the deformation of the blade are balanced between both sides of the blade in such a way that the deformation equals to zero. Nevertheless, the method disregards the structural mechanics of the part that, for instance, includes the geometrical moment of inertia. This provides different behavior of the part depending on the point of load.

The process for each side may be divided into several points of load along the tool path. Due to the bigger spread of the survey on blade side 2, the points of load lie closer to the edges of the blade, which causes a difference in the equivalent load compared to the opposite side and therefore a part deformation unequal to zero after re-contouring.

Same is the reason for the forecast error in the prediction of part distortion depicted in Fig. 1. However, the impact of this effect is not as significant as the balance of the equilibration of the internal loads. That is the reason for the successful compensation of the part distortion for blade 2. Quantitatively, the results reveal a maximum part distortion of $\Delta PV = 22$ µm for blade 1 and $\Delta PV = 28$ µm for blade 2. This is an improvement of shape accuracy of 21% compared to a conventional strategy.

5. Conclusion

This paper presents a novel method for the compensation of part distortions within process planning for re-contouring of thin-walled workpieces. The technique includes an optimization of tool angles in 5-axis re-contouring. It is based on the re-contouring areas as well as the simulated surface generating cut volume (SGCV). The second part of the method relates to the safe implementation of the tool angles in an automatic tool path modification. The re-contouring of two blades shows that the method allows a compensation of part distortion of 21% compared to a conventional process. Currently, the method is based on the equilibrium of internal loads. In future work, the structural mechanics of the part will be taken into account in order to improve the accuracy of the method.

Acknowledgements

The authors thank the German Research Foundation (DFG) for the financial support within the Collaborative Research Center 871: Regeneration of complex capital goods as well as the Institute of Materials Science (IW) for the heat treatment of the workpieces.

References

[1] Michaels K. MRO Industry Outlook. Montréal; 28 April 2016.
[2] Gao J, Chen X, Yilmaz O, Gindy N. An integrated adaptive repair solution for complex aerospace components through geometry reconstruction. Int J Adv Manuf Technol 2008;36(11-12):1170–1179.
[3] Mohaghegh K, Sadeghi MH, Abdullah A. Reverse engineering of turbine blades based on design intent. Int J Adv Manuf Technol 2007;32(9-10):1009–1020.
[4] Yilmaz O, Gindy N, Gao J. A repair and overhaul methodology for aeroengine components. Robotics and Computer-Integrated Manufacturing 2010;26(2):190–201.
[5] Tao W, Huapeng D, Jie T, Hao W. Recent Repair Technology for Aero-Engine Blades. Recent Patents on Engineering 2015;9(2):132–141.
[6] Wu B, Wang J, Zhang Y, Luo M. Adaptive location of repaired blade for multi-axis milling. J Comp Des Eng 2015;2(4):261–267.
[7] Wu H, Gao J, Li S, Zhang Y, Zheng D. A Review of Geometric Reconstruction Algorithm and Repairing Methodologies for Gas Turbine Components. Telkomnika 2013;11(3):1609–1618.
[8] Böß V, Denkena B, Wesling V, Kaierle S, Rust F, Nespor D, Rottwinkel B. Repairing parts from nickel base material alloy by laser cladding and ball end milling. Prod Eng Res Devel 2016;10(4-5):433–441.
[9] Chen HC, Pinkerton AJ, Li L. Fibre laser welding of dissimilar alloys of Ti-6Al-4V and Inconel 718 for aerospace applications. Int J Adv Manuf Technol 2011;52(9-12):977–987.
[10] Leyens C, Beyer E. Innovations in laser cladding and direct laser metal deposition. In: Laser Surface Engineering. Elsevier; 2015. p.181–192.
[11] Wilson JM, Piya C, Shin YC, Zhao F, Ramani K. Remanufacturing of turbine blades by laser direct deposition with its energy and environmental impact analysis. J Clean Prod 2014;80:170–178.
[12] Gao J, Chen X, Zheng D, Yilmaz O, Gindy N. Adaptive restoration of complex geometry parts through reverse engineering application. Adv Eng Softw 2006;37(9):592–600.
[13] Yilmaz O, Noble D, Gindy N. A study of turbomachinery components machining and repairing methodologies. Aircraft Engineering and Aerospace Technology: An International Journal 2005;77/6:455–466.
[14] Wang MH, Sun Y. Error prediction and compensation based on interference-free tool paths in blade milling. Int J Adv Manuf Technol 2014;71(5-8):1309–1318.
[15] Gang L. Study on deformation of titanium thin-walled part in milling process. J Mat Process Technol 2009;209(6):2788–2793.
[16] Zhan C, Yang W. A high efficient surface-based method for predicting part distortions in machining and shot peening. Int J Mech Sci 2016;119:125–143.
[17] Denkena B, Grove T, Mücke A, Langen D, Nespor D, Hassel T. Residual stress formation after re-contouring of micro-plasma welded Ti−6Al−4 V parts by means of ball end milling. Mat.-wiss. u. Werkstofftech 2017;48(11):1034–1039.
[18] Denkena B, Mücke A, Schumacher T, Langen D, Hassel T. Technology-Based Recontouring of Blade Integrated Disks After Weld Repair, J Eng Gas Turb Power 2018; 140:121015/1-121015/8.
[19] Böß V, Ammernann C, Niederwestberg D, Denkena, B. Contact Zone Analysis Based on Multidexel Workpiece Model and Detailed Tool Geometry Representation. Procedia CIRP 2012;4:41–45.
[20] Denkena B, Nespor D, Böß V, Köhler J. Residual stresses formation after re-contouring of welded Ti-6Al-4V parts by means of 5-axis ball nose end milling. J Manufact Sci Technol 2014;7(4):347–360.